



# CXCR7 promotes the migration of fibroblasts derived from patients with acquired laryngotracheal stenosis by NF- $\kappa$ B signaling

Mengrou Xu<sup>1#</sup>, Bin Hu<sup>2#</sup>, Jiarui Chen<sup>1</sup>, Limin Zhao<sup>1</sup>, Jing Wang<sup>1^</sup>, Xiaoyan Li<sup>1^</sup>

<sup>1</sup>Department of Otorhinolaryngology Head and Neck Surgery, Shanghai Children's Hospital, Shanghai Jiao Tong University School of Medicine, Shanghai, China; <sup>2</sup>Department of Otorhinolaryngology Head and Neck Surgery, Changhai Hospital Affiliated with the Second Military Medical University of PLA, Shanghai, China

**Contributions:** (I) Conception and design: M Xu, B Hu; (II) Administrative support: J Wang, X Li; (III) Provision of study materials or patients: L Zhao; (IV) Collection and assembly of data: J Chen; (V) Data analysis and interpretation: J Wang, X Li; (VI) Manuscript writing: All authors; (VII) Final approval of manuscript: All authors.

<sup>#</sup>These authors contributed equally to this work.

**Correspondence to:** Xiaoyan Li, MD, PhD; Jing Wang, MD, PhD. Department of Otorhinolaryngology Head and Neck Surgery, Shanghai Children's Hospital, Shanghai Jiao Tong University School of Medicine, No. 355, Luding Road, Shanghai 200062, China. Email: xiaoyanli\_2014@163.com; wangjing80s@163.com.

**Background:** Laryngotracheal stenosis (LTS) is a life-threatening disease that commonly results in airway obstruction in children. Traditional treatments such as laryngotracheal reconstruction and balloon dilation all have the risk of laryngotracheal restenosis. It is of great importance to spare patients the morbidity of LTS and risks of restenosis associated with these treatments. Laboratory and clinical trials have focused on fibrosis, the crucial pathological process of LTS. This study was undertaken to investigate the function of CXC chemokine receptor-7 (*CXCR7*) in the fibroblasts derived from LTS.

**Methods:** RNA sequencing was performed on acquired human LTS and normal trachea tissues to analyze differentially expressed genes. Fibroblasts from LTS and normal trachea tissues were isolated and cultured. *CXCR7* knockdown was performed using specific small interfering RNAs (siRNAs) and activated by *CXCR7* agonist VUF11207. The assessment of cell proliferation and migration was conducted using EdU proliferation, wound healing, and transwell assays. The assessment of cell proliferation and migration was conducted using EdU proliferation, wound healing, and transwell assays. The expressions of *CXCR7*, *E-cadherin* and NF- $\kappa$ B signaling pathway were analyzed by quantitative polymerase chain reaction (qPCR), western blotting, immunohistochemistry, and immunofluorescence.

**Results:** RNA sequencing showed that *CXCR7* was among the most differentially expressed genes. LTS had an increased *CXCR7* expression but decreased *E-cadherin* expression *in vivo*. *CXCR7* agonist stimulated the migration of LTS derived fibroblasts significantly *in vitro*, with no significant influence on the cell proliferation and apoptosis. *CXCR7* agonist inhibited the expression of *E-cadherin* by activating the NF- $\kappa$ B signaling pathway. The effects of *CXCR7* on cell migration and *E-cadherin* expression were blocked by *CXCR7* siRNA.

**Conclusions:** LTS had an increased *CXCR7* expression but decreased *E-cadherin* expression. *CXCR7* activation inhibited *E-cadherin* expression by NF- $\kappa$ B signaling pathway and thereby promoted the migration of LTS derived fibroblasts.

**Keywords:** CXC chemokine receptor-7 (*CXCR7*); migration; laryngotracheal stenosis (LTS); fibrosis

<sup>^</sup> ORCID: Xiaoyan Li, 0000-0002-8874-5634; Jing Wang, 0000-0003-3292-6521.

Submitted Feb 25, 2023. Accepted for publication Aug 02, 2023. Published online Sep 14, 2023.

doi: 10.21037/tp-23-118

View this article at: <https://dx.doi.org/10.21037/tp-23-118>

## Introduction

Laryngotracheal stenosis (LTS) is a life-threatening disease that causes breathing difficulties and seriously impacts the quality of life, especially in children. Minimally invasive treatments, such as balloon dilation, and surgical therapies, such as end-to-end anastomosis and reconstruction, can effectively alleviate laryngeal obstruction symptoms but may have many complications (1). The prevention and treatment of postoperative complications is a major clinical problem. The crucial pathological process of LTS is fibrosis, which includes dysregulated fibroblast proliferation, migration, myofibroblast activation and abnormal extracellular matrix (ECM) deposition (2-4). Molecular mechanisms of fibrosis are being targeted to attenuate fibrosis in laboratory and clinical trials, such as TGF- $\beta$  antagonist (5). Previous articles have mainly focused on inhibiting excessive deposition of ECM and associated signaling pathways.

Recently, fibroblast and fibrosis heterogeneity have been found by single-cell RNA sequencing technology (6,7). It was revealed that fibroblasts from different anatomic sites have different transcriptional profiles and cell behaviors (8,9). So, the characteristics of LTS derived fibroblasts should be researched.

In our last work, we revealed the heterogeneity of fibroblasts between LTS and skin hypertrophic scar in pediatric patients (10). We found that fibroblasts derived from LTS demonstrated significantly faster cell proliferation and migration rates. The expression of CXC chemokine receptor-7 (*CXCR7*) was significantly higher in the fibroblasts of LTS than skin hypertrophic scar. But lower expression of Col1a1 and  $\alpha$ -SMA in fibroblasts of LTS were identified, which we hypothesized that may be resulted from the effect of *CXCR7*. The functions of *CXCR7* were mostly studied in the endothelial cells. A study reported that TGF- $\beta$ 1 could induce *CXCR7* expression in lung endothelial cells (11). Overexpression of *CXCR7* was found to decrease TGF- $\beta$ 1-induced collagen production and the expression of  $\alpha$ -SMA by blocking the Jag1-Notch pathway. Inhibition of *CXCR7* induced persistent upregulation of the Jag1-Notch signaling pathway (12). In human umbilical vein endothelial cells, *CXCR7* knockdown was found to inhibit the cell proliferation. *CXCR7* overexpression inhibited  $\alpha$ -SMA expression (13), which is consistent with our findings. In the oral fibroblasts, *CXCR7* was found to stimulate cell migration (14). In cancer cells, *CXCR7* inhibition decreased the migration of cancer stem cells (15). In the head and neck squamous cell carcinoma cells, *CXCR7* overexpression was also found to enhance the cell migration (16). So, *CXCR7* was shown to be related with cell proliferation and migration. However, the functions of *CXCR7* in fibroblasts of LTS have not been reported yet.

Thus, this study aims to investigate the role of *CXCR7* in the fibroblasts derived from the LTS tissues. We characterized the expression of *CXCR7* by RNA sequencing of LTS and studied the effects of *CXCR7* on the expression of *E-cadherin* and migration of fibroblasts of LTS. We found out that *CXCR7* inhibits the expression of *E-cadherin* and promotes fibroblast migration by NF- $\kappa$ B signaling pathway. We present this article in accordance with the MDAR reporting checklist (available at <https://tp.amegroups.com/>)

### Highlight box

#### Key findings

- LTS had an increased *CXCR7* expression but decreased E-cadherin expression *in vivo* and *in vitro* fibroblasts.
- *CXCR7* agonist could inhibit E-cadherin expression by activating NF- $\kappa$ B signaling pathway and thereby promotes LTS derived fibroblasts' migration, which may contribute to the pathogenesis of fibrosis in LTS.

#### What is known and what is new?

- The heterogeneity of fibroblasts exists between LTS and skin hypertrophic scar in pediatric patients. Specifically, fibroblasts derived from LTS demonstrated significantly faster cell proliferation and migration rates, compared to those from skin hypertrophic scars. The expression of *CXCR7* was significantly higher in the fibroblasts from LTS than in those from skin hypertrophic scar.
- *CXCR7* may have an effect on the expression of E-cadherin and migration of fibroblasts of LTS. *CXCR7* inhibits the expression of E-cadherin and promotes fibroblast migration by NF- $\kappa$ B signaling pathway.

#### What is the implication, and what should change now?

- LTS may have an increased *CXCR7* expression, which could inhibit E-cadherin expression by NF- $\kappa$ B signaling pathway and thereby promotes the migration of LTS derived fibroblasts. *CXCR7* are expected to become a promising target for the treatment of LTS.

article/view/10.21037/tp-23-118/rc).

## Methods

### Cell isolation and culture

Twelve patients (5 boys and 7 girls) were diagnosed with LTS and underwent the tracheal resection and T-shaped tracheal stent implantation surgery in Shanghai Children's Hospital (Shanghai, China) from September 2019 to October 2020. Age at surgery ranged from 36 to 61 months (median age of 45 months). LTS tissues (n=12) and normal trachea tissues on the edge of them (n=12) were obtained from these patients. The specimens were washed three times with sterile 1× PBS and then treated with a 0.25% Collagenase I solution at 37 °C. The mixtures were filtered with sterile 70-µm strainer. Fibroblasts were cultured in high sugar Dulbecco's Modified Eagle Medium (Hyclone, Thermo Fisher Scientific, Waltham, MA, USA) supplemented with 15% fetal bovine serum (Hyclone, Thermo Fisher Scientific, Waltham, MA, USA), 100 U/mL penicillin, and 100 mg/L streptomycin. Fibroblasts were incubated at 37 °C with 5% CO<sub>2</sub> in a humidified atmosphere. Primary fibroblasts of passages 2–6 were used.

The study was conducted in accordance with the Declaration of Helsinki (as revised in 2013). The study was approved by Committees of human ethics and experimental safety of Shanghai Children's Hospital (No. 2019R065) and informed consent was taken from the patients' guardians.

### RNA sequencing

LTS and normal trachea samples were acquired. RNA quantity was measured on a NanoDrop instrument (Thermo Fisher Scientific, Waltham, MA). The cDNA library was constructed using KAPA RNA-Seq Library Preparation Kit (Illumina, San Diego, CA). The cDNA samples sequencing was performed on an Illumina HiSeq 4000 sequencing platform. Raw data were analyzed using Illumina/Solexa Pipeline (Off-Line Base Caller software). The Gene Ontology (GO) and Kyoto Encyclopedia of Genes and Genomes (KEGG) pathway enrichment analysis was performed for differentially expressed genes using the Database of Kyoto Encyclopedia of Genes and Genomes online tools (<http://www.genome.jp/kegg>). Hierarchical cluster analysis was performed by GeneSight-Lite 4.1.6 (BioDiscovery, El Segundo, CA, USA). The protein-protein interaction network and co-expression of the proteins

encoded by the differentially expressed genes was analyzed by the GeneMANIA Cytoscape.

### Quantitative PCR

Total RNA was extracted using TRIzol (Invitrogen) according to the manufacturer's instructions. RNA concentrations were examined using the NanoDrop (ND-8000; Thermo Fisher Scientific). RNAs were reverse-transcribed into cDNA using the Moloney murine leukemia virus reverse transcriptase (M-MLV) system (Promega Biotech, Madison, WI, USA). Quantitative PCR (qPCR) was performed with an ABI 7900HT (Applied Biosystems, Foster City, CA, USA) system using SYBR Premix (Takara, Dalian, China). Glyceraldehyde-3-phosphate dehydrogenase (GAPDH) was used as the internal control. The data were analyzed using the comparison Ct ( $2^{-\Delta\Delta C_t}$ ) method and expressed as the fold change relative to the respective control. The primer sequences used in this study were as follows: *GAPDH*: forward, 5'-AGGTCGGTGTGAACGGATTTG-3'; reverse, 5'-GGGGTTCGTTGATGGCAACA-3'; *Cxcr7*: forward, 5'-TCTGCATCTCTTCGACTACTCA-3'; reverse, 5'-GTAGAGCAGGACGCTTTTGT-3'. *E-cadherin*: forward, 5'-TCATGATGCTACCCGAGGTTTG-3'; reverse, 5'-CAGAACTAGATGCAGCCGGAGA-3'.

### Immunohistochemistry and immunofluorescence

After being fixed in 10% paraformaldehyde and embedded in paraffin, the specimens were cut into 5-µm-thick sections and then stained with primary antibodies against CXCR7 (1:200; Cat:ab138509; Abcam, Cambridge, United Kingdom) and E-cadherin [1:200; Cat:3195; Cell Signaling Technology (CST), Danvers, MA, USA] at 4 °C overnight. Secondary antibodies were used at room temperature for 30 min. The percentage of positive cells was analyzed with the ImageJ software (Image J; NIH, Bethesda, MD, USA).

For immunofluorescence, after fixed by 4% paraformaldehyde for 30 min, then permeabilized by 0.1% Triton X-100 for 30 min, cells were blocked with 5% bovine serum albumin (BSA) and goat serum at room temperature for 60 min. Anti-E-cadherin (1:200; Cat:3195; CST, Danvers, MA, USA) and P65 (1:200, Novus Biologicals, Centennial, CO) antibodies were used overnight at 4 °C, followed by an Alexa Fluor 488 or 555-conjugated secondary antibody. Cells were visualized by a confocal microscope (Leica, Solms, Germany).

### Western blotting

Whole-cell protein lysates were lysed with radioimmunoprecipitation (RIPA) buffer containing a protease inhibitor cocktail (Roche, Basel, Switzerland). The concentrations of protein were measured by the bicinchoninic acid (BCA) assay (Thermo Fisher Scientific). Then, 40 µg protein lysate per sample was separated by 10% or 12% sodium dodecyl sulfate-polyacrylamide gel electrophoresis (SDS-PAGE) and transferred to 0.45-µm polyvinylidene difluoride membranes using a semi-dry transfer system (Trans-Blot Turbo; Bio-Rad Laboratories, Hercules, CA, USA). The membranes were incubated overnight at 4 °C with primary antibodies and then incubated with horseradish peroxidase-conjugated secondary antibody (1:4,000; Cat:7074; CST, Danvers, MA, USA). The secondary antibody was used and visualized using an electrochemiluminescence kit (Tanon Science & Technology, Shanghai, China), and a chemiluminescence imaging system (6100; Tanon Science & Technology). The antibodies used in this study were as follows: anti-phospho-ERK (1:2,000; Cat:4370; CST, Danvers, MA, USA), anti-ERK (1:2,000; Cat:4695; CST, Danvers, MA, USA); anti-phospho-P65 (1:1,000; Cat:3033; CST, Danvers, MA, USA), anti-P65 (1:1,000; Cat:8242; CST, Danvers, MA, USA); anti-CXCR7 (1:1,000; Cat:ab138509; Abcam, Cambridge, United Kingdom); anti-E-cadherin (1:1,000; Cat:3195; CST, Danvers, MA, USA).

### EdU incorporation assay

Cell proliferation was determined by a EdU (5-ethynyl-2'-deoxyuridine) Cell Proliferation Assay Kit (Invitrogen, Click-iT® EdU Imaging Kits) according to the manufacturer's protocol. Cells were incubated with EdU for 2 h, fixed by 4% paraformaldehyde (PFA) for 10 min, and treated by a Click-iT EdU reaction cocktail for 30 min. Cell nuclei were stained with 4',6-diamidino-2-phenylindole (DAPI, 1:1,000; Sigma-Aldrich) for 10 min. The proportion of EdU positive cells was analyzed by Zeiss 710 laser-scanning microscope (Zeiss, Thornwood, NY, USA).

### Cell migration assays

Cells were cultured in six-well plates. When fibroblasts grow 90% confluence, straight scratches were created in each well. Then, fibroblasts were treated with CXCR7 agonist or DMSO. The middle gap areas were observed and measured using ImageJ software (NIH, Bethesda, MD,

USA) at 0, 24 and 48 hours.

For transwell assay, cells were cultured on the top transwell membranes of 24-well plates with 8 mm pore size polycarbonate transwell culture inserts (Corning, NY). CXCR7 agonist or DMSO was added to the lower chambers. After incubation, the membranes of transwell were removed and fixed. Migrated cells on the lower surface were stained with 0.5% crystal violet for several minutes. We used ImageJ software to count and measure the number of cells that migrated to the lower surface of the membrane.

### siRNA knockdown studies

To transfect small interfering RNA (siRNA) oligos, Lipofectamine RNAiMAX reagent (Invitrogen, Carlsbad, CA) was used following the manufacturer's instructions. The fibroblasts were transfected with 100 nM CXCR7 siRNA (SR311311, SR324637, OriGene Technologies, Rockville, MD) in 6-well plates. Scramble siRNA (sc-37007) was used as control.

### Statistical analysis

The western blots and immunohistochemistry results were quantified by ImageJ software. Statistical software package SPSS 20.0 (SPSS, Chicago, IL, USA) was used with the Mann-Whitney non-parametric test or the Student's *t*-test. The results were presented as means ± standard deviation (SD). Significant differences were defined as P value less than 0.05. All experiments were repeated at least three times.

## Results

### The expressions of CXCR7 and E-cadherin in LTS in vivo

In our previous work (10), we found that the expression of CXCR7 were significantly increased in LTS. So, first, RNA sequencing was performed in acquired human LTS and normal trachea tissues to analyze differentially expressed genes and identify genes associated or co-expressed with CXCR7. Differentially expressed genes were visualized by heatmaps and gene-rank maps, which showed that CXCR7 was among the most up-regulated genes. GO and KEGG enrichment analysis found that differentially expressed genes were enriched in cell migration, cell adhesion, cytokine-mediated signaling pathway and NF-κB signaling pathway. The protein-protein interaction network and co-expression analysis showed that CXCR7 may co-expression with E-cadherin (Figure 1A). Next, we tried to investigate the

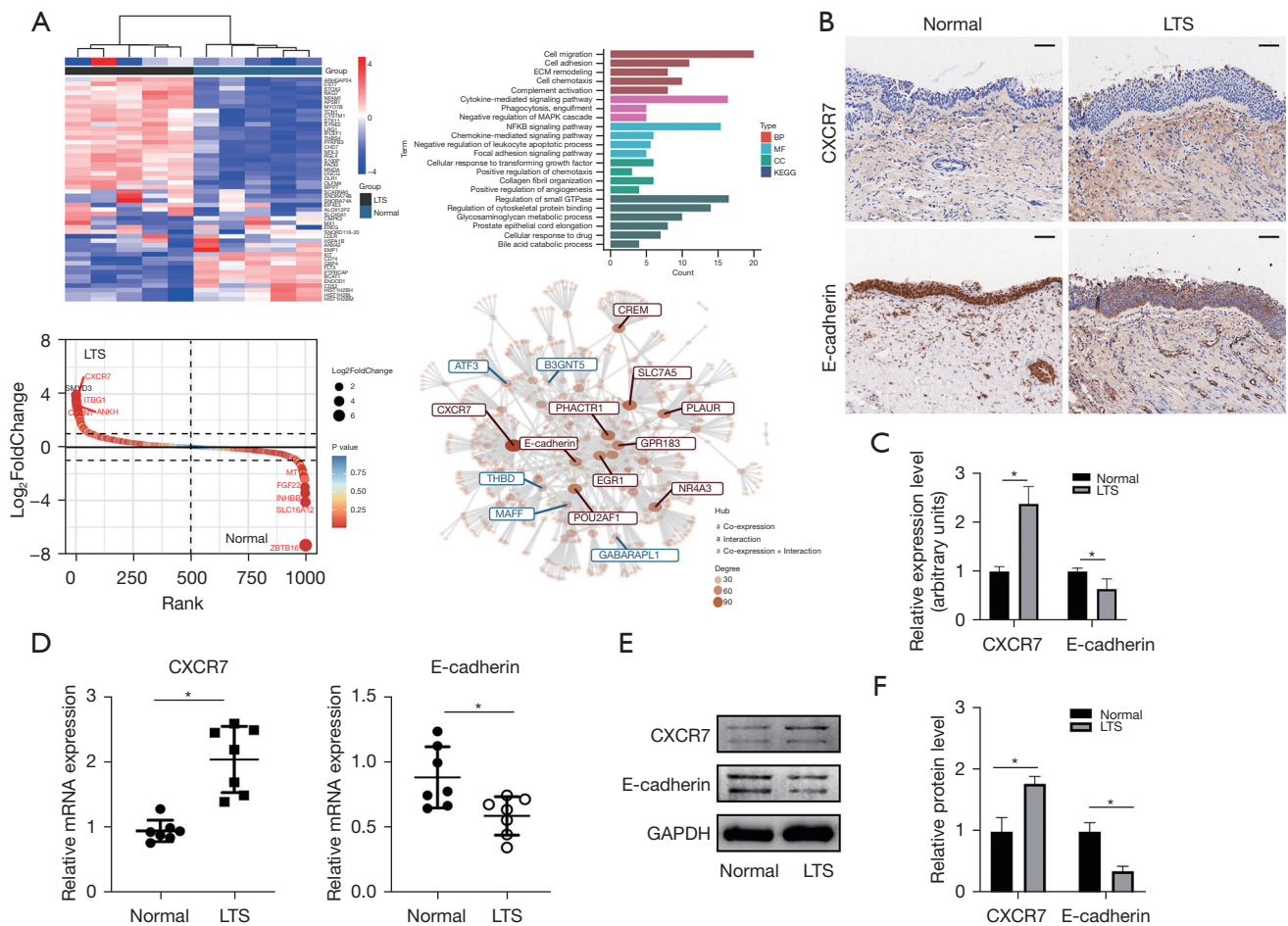


**Figure 1** The expressions of CXCR7 and E-cadherin in LTS *in vivo*. (A) Heatmap, GO analysis, different gene expression analysis, and the protein-protein interaction network analysis of the transcriptomes of fibroblasts from the normal trachea and LTS. (B) Representative images of the normal trachea and LTS with IHC staining indicating CXCR7 and E-cadherin positive cells. Scale bars, 100  $\mu$ m. (C) Quantification of the expressions of CXCR7 and E-cadherin in IHC.  $n \geq 3$ . (D) The relative mRNA expressions of CXCR7 and E-cadherin were measured using qPCR in normal trachea and LTS. (E) The protein expressions of CXCR7 and E-cadherin were measured and quantified (F) by western blot. Data were mean  $\pm$  SD;  $n \geq 3$ ; \*,  $P < 0.05$ . CXCR7, CXC chemokine receptor-7; LTS, laryngotracheal stenosis; BP, biological progress; CC, cellular component; MF, molecular function; KEGG, Kyoto Encyclopedia of Genes and Genomes; GO, Gene Ontology; IHC, immunohistochemical; qPCR, quantitative polymerase chain reaction; SD, standard deviation.

expression of CXCR7 and E-cadherin in human LTS and normal trachea tissue *in vivo*. By immunohistochemistry, LTS showed an increased CXCR7 but decreased E-cadherin staining (Figure 1B, and the staining results were quantified in Figure 1C), which were consistent with our previous results (10) and the data of RNA sequencing. By qPCR and western blot, LTS showed an increased CXCR7 but decreased E-cadherin expression (Figure 1D-1F). These above results showed that LTS showed an increased CXCR7 expression, which may regulate the expression of E-cadherin.

### CXCR7 agonist promoted cell migration of LTS derived fibroblasts *in vitro*

To study the functions of CXCR7 in LTS, human LTS derived fibroblasts were isolated and cultured. Fibroblasts of passages 2–6 were used. The effect of CXCR7 agonist VUF11207 on cell proliferation were analyzed by cell count and EdU incorporation assay. The results showed that CXCR7 had no effect on fibroblast proliferation (Figure 2A,2B). By PI–annexin V fluorescence-activated cell sorting analysis, there was no significant difference

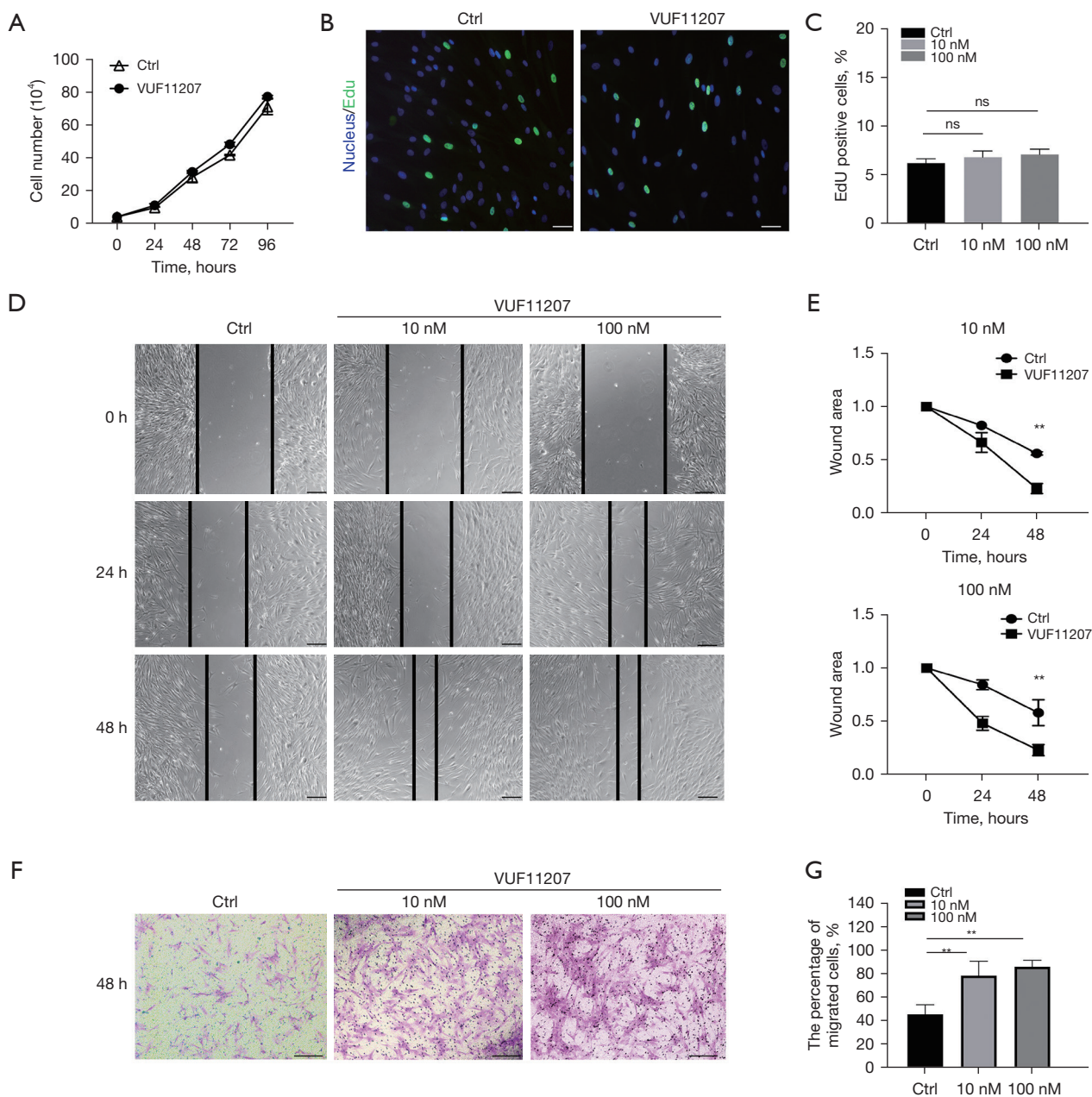


**Figure 2** CXCR7 agonist promoted cell migration of LTS derived fibroblasts *in vitro*. (A) Cell number counts of human LTS derived fibroblasts treated by CXCR7 agonist VUF11207. (B) EdU (green) was used to label proliferating cells treated by CXCR7 agonist VUF11207. Scale bars, 50  $\mu$ m. The percentages of EdU-positive cells were also quantified (C). (D) Representative images of the wound-healing assay of LTS derived fibroblasts treated by VUF11207 in 24 and 48 hours. The wound areas are indicated by black full lines. Scale bars, 100  $\mu$ m. (E) Quantification of the wound areas in (D). (F) Culture medium with different concentrations of VUF11207 (10 and 100 nM) were applied to measure LTS derived fibroblasts. Migrated cells on the lower surface were stained with 0.5% crystal violet for several minutes. Scale bars, 100  $\mu$ m. (G) Quantification of the percentages of cell migration in (F). Data were mean  $\pm$  SD;  $n \geq 3$ ; \*\*,  $P < 0.01$ ; ns, not significant. CXCR7, CXC chemokine receptor-7; LTS, laryngotracheal stenosis; EdU, 5-ethynyl-2'-deoxyuridine; SD, standard deviation.

of the apoptotic cells after CXCR7 agonist treatment (Figure 2C). Then, wound healing assay and transwell assay were used to investigate the migration ability. The result showed that the gap area of the wound was smaller after treated by CXCR7 agonist (10 and 100 nM) for 48 hours (Figure 2D,2E). The transwell assay also found that CXCR7 agonist induced more migrated fibroblast to the lower surface of the transwell membrane (Figure 2F,2G). These above results indicated that CXCR7 agonist promoted cell migration of LTS derived fibroblasts *in vitro*, but not proliferation.

### ***CXCR7 inhibited E-cadherin expression and promoted fibroblast migration through activating NF-κB signaling pathway***

Then, we tried to explore which signaling pathway CXCR7 activated to promote fibroblast migration. It was reported that CXCR7 may enhance the migration of head and neck squamous cell carcinoma cells by upregulating TGF-β1/Smad2/3 (16) and NF-κB (17) signaling pathways. E-cadherin plays an essential role in controlling cell migration (18,19). The mRNA expressions of CXCR7 and E-cadherin were examined by qPCR. The results showed that the mRNA expressions of E-cadherin were clearly down-regulated in CXCR7 agonist treated fibroblasts, while CXCR7 expression was unchanged (Figure 3A). The decreased expression of E-cadherin in CXCR7 agonist treated fibroblasts was further confirmed by E-cadherin immunofluorescence and western blot assay (Figure 3B,3C). Next, the protein expressions of ERK and NF-κB signaling pathways were analyzed. The protein expressions of ERK and phosphorylated ERK were not significantly changed after CXCR7 agonist treatment. After CXCR7 agonist treatment (10 or 100 nM), the expression of phosphorylated P65 (a subunit of nuclear factor NF-κB) was up-regulated (Figure 3C,3D). By immunostaining of P65, P65 was shown to translocate into nuclear after CXCR7 agonist treatment, which indicated that CXCR7 activated NF-κB signaling pathway (Figure 3E).

To confirm the role of CXCR7 in regulating E-cadherin expression and fibroblast migration, we inhibited CXCR7 expression by specific siRNAs and investigated the E-cadherin expression, NF-κB signaling pathway and fibroblast migration. Two siRNAs were used to inhibit the expression of CXCR7. The inhibitory effect of siRNAs was shown by qPCR and western blot assay (Figure 4A,4B). Next, we treated fibroblasts with CXCR7 siRNA and

CXCR7 agonist. The results showed that CXCR7 agonist inhibited E-cadherin mRNA and protein expressions were rescued by CXCR7 siRNA significantly (Figure 4C-4E). The results of wound healing assay and transwell assays showed that CXCR7 agonist promoted fibroblast migration was inhibited by CXCR7 siRNA (Figure 4F,4G). Furthermore, NF-κB signaling pathway was examined by immunofluorescence, which showed that CXCR7 agonist activated P65 nuclear translocation decreased obviously by CXCR7 siRNA (Figure 4H). Taken together, we identified that CXCR7 inhibited E-cadherin expression by NF-κB signaling pathway and thereby promoted LTS derived fibroblast migration (Figure 5).

### **Discussion**

Growing evidence showed that CXCR7 may regulate fibroblast proliferation and migration. It has been observed that CXCR7 promoted fibroblast migration in oral fibroblasts, but not proliferation (14). In lung adenocarcinoma, knockdown of CXCR7 inhibited the cell migration (15). Overexpression of CXCR7 increased human umbilical vein endothelial cells migration (13). Furthermore, CXCR7 overexpression was discovered to increase the migration ability of squamous cell carcinoma cells (16). CXCR7 blocking inhibited the migration of macrophages in the synovial tissues (20). By structural complementation assay using NanoBiT technology, SDF-1α was found to stimulate cell migration mediated by both CXCR4 and CXCR7 (21). So, CXCR7 was positively correlated with the migration of fibroblasts and other cells. Based on our previous data, we observed a decrease in the expression of E-cadherin in LTS, and we speculated that CXCR7 may regulate fibroblast migration by down-regulating E-cadherin expression (10). E-cadherin plays an essential role in controlling cell migration (18,19). In this work, we demonstrated that CXCR7 agonist stimulated the migration of LTS derived fibroblasts significantly *in vitro*, with no significant influence on the cell proliferation and apoptosis. Besides, we discovered that CXCR7 agonist inhibited E-cadherin expression was rescued by CXCR7 siRNA significantly. So, we confirmed the role of CXCR7 in regulating E-cadherin expression and LTS derived fibroblast migration.

In this work, we also revealed that the downstream NF-κB signaling pathway was activated by CXCR7. It has been reported that CXCR7 could activate ERK, NF-κB, Wnt/β-Catenin, TGF-β/Smad (11,15,16) or Jag1-Notch (12)

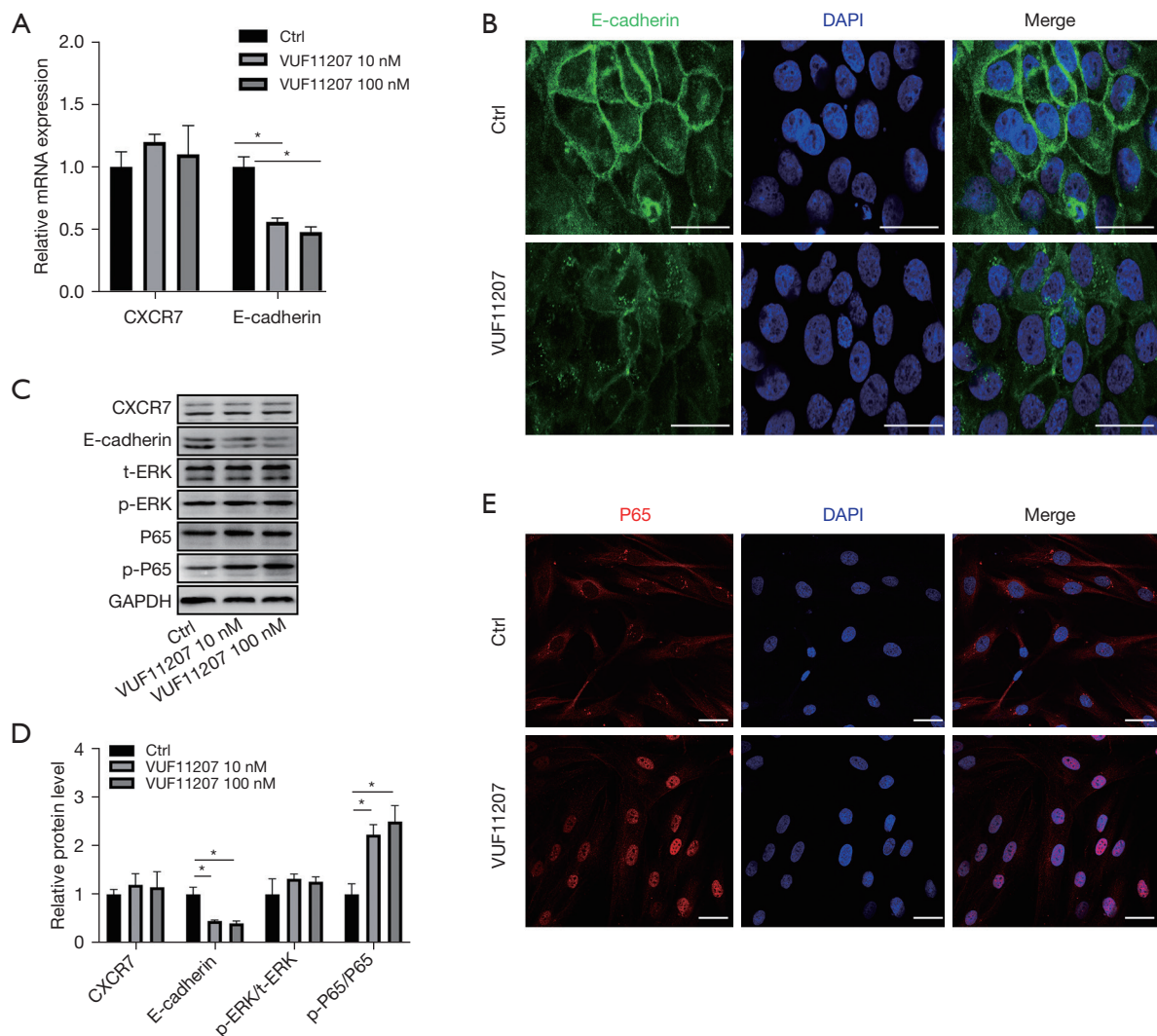


**Figure 3** CXCR7 agonist inhibited E-cadherin expression and activated NF- $\kappa$ B signaling pathway *in vitro*. (A) The relative mRNA expressions of *CXCR7* and *E-cadherin* were measured by qPCR in human LTS derived fibroblasts treated by CXCR7 agonist VUF11207. (B) Immunostaining of E-cadherin (green) expression in LTS derived fibroblasts treated by CXCR7 agonist, compared with control cells. Scale bar, 50  $\mu$ m. (C) The protein expressions of CXCR7, E-cadherin, total-ERK, phospho-ERK, P65 and phospho-P65 were measured by western blot. The expression of GAPDH was utilized as an internal control. (D) Quantification of protein expressions in (C). (E) Immunostaining of P65 (red) and nuclear (blue) location in LTS derived fibroblasts treated by CXCR7 agonist, compared with control cells. Scale bar, 50  $\mu$ m. Data were mean  $\pm$  SD;  $n \geq 3$ ; \*,  $P < 0.05$ . CXCR7, CXC chemokine receptor-7; qPCR, quantitative polymerase chain reaction; LTS, laryngotracheal stenosis; GAPDH, glyceraldehyde 3-phosphate dehydrogenase; SD, standard deviation.

signaling pathway. By using siRNA knockdown, *CXCR7* was shown to activate downstream  $\beta$ -arrestin dependent cell signaling pathways, including ERK, p38 MAPK, and SAPK (22). In endothelial progenitor cells, shear stress stimulation increased the *CXCR7* expression and induced ERK signaling pathways (23). However, in our results, ERK signaling did not significantly changed after *CXCR7* agonist

or siRNA knockdown treatment in the fibroblasts from LTS. In pulmonary endothelial cells, *CXCR7* expression was increased and activated NF- $\kappa$ B signaling pathway (24). In human vascular endothelial cell line, *CXCR7* inhibition blocked the phosphorylation of IKK and I $\kappa$ B and nuclear translocation of NF- $\kappa$ B P65 (25). *CXCR7* enhanced the expression of tight junctions by inducing



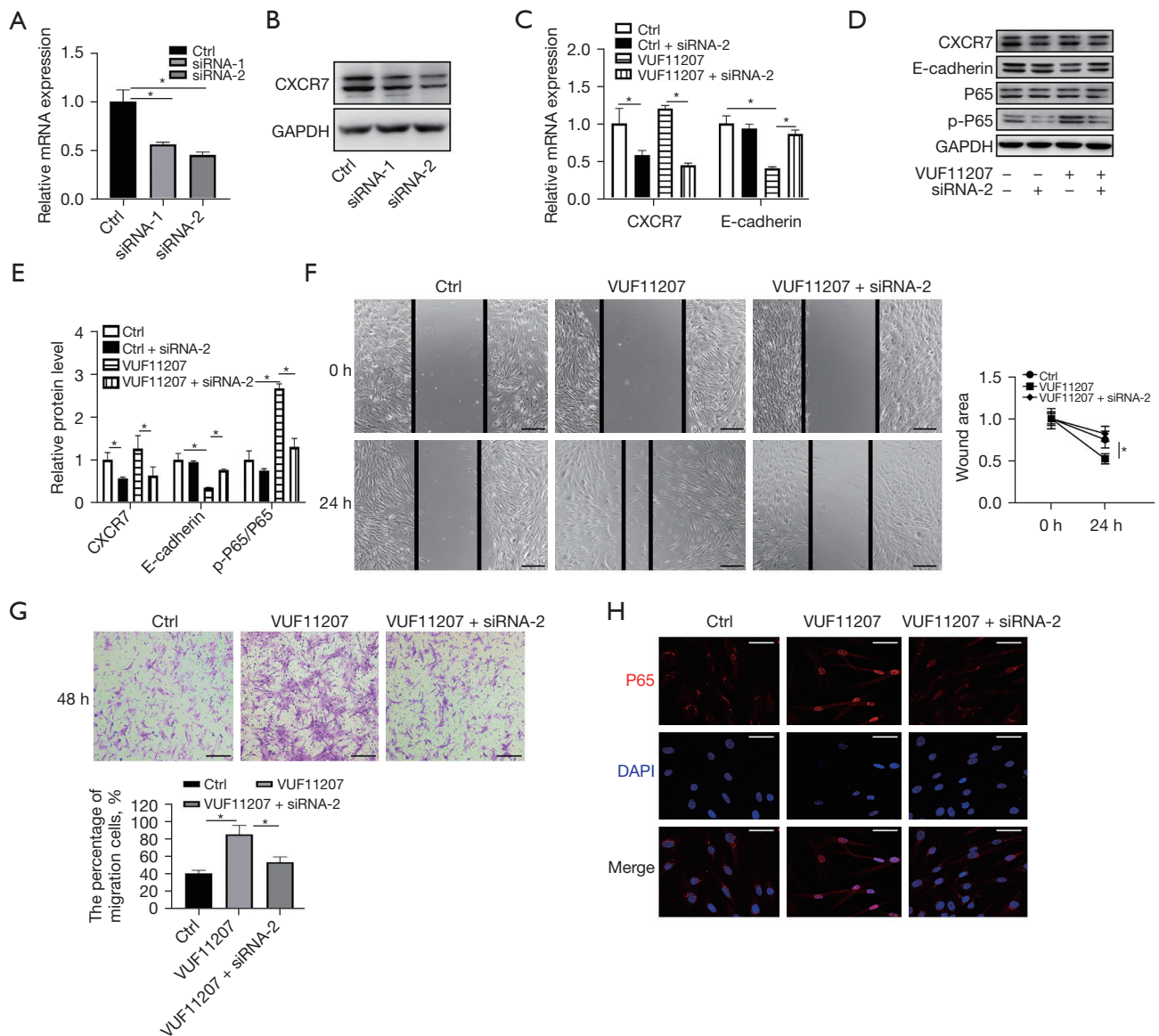


**Figure 4** CXCR7 inhibited *E-cadherin* expression and promoted fibroblast migration through activating NF- $\kappa$ B signaling pathway. (A) The relative mRNA and protein (B) expression of CXCR7 after treatment of specific siRNAs of CXCR7. (C) The relative mRNA expressions of CXCR7 and *E-cadherin* were measured by qPCR after treatment of CXCR7 agonist VUF11207 and CXCR7 siRNA. (D) The protein expressions of CXCR7, *E-cadherin*, P65 and phospho-P65 were measured by western blot after treatment of CXCR7 agonist VUF11207 and CXCR7 siRNA. GAPDH expression was used as an internal control. (E) Quantification of the protein expressions in (D). (F) Representative images of the wound-healing assay of LTS derived fibroblasts treated by VUF11207 and CXCR7 siRNA. The wound areas are indicated by black full lines. Scale bars, 100  $\mu$ m. (G) Cell migration assay of LTS derived fibroblasts treated by VUF11207 and CXCR7 siRNA. Migrated cells on the lower surface were stained with 0.5% crystal violet for several minutes. Scale bars, 100  $\mu$ m. (H) Immunostaining of P65 (red) and nuclear (blue) location in LTS derived fibroblasts treated by CXCR7 agonist and siRNA, compared with control cells. Scale bar, 50  $\mu$ m. Data were mean  $\pm$  SD;  $n \geq 3$ ; \*,  $P < 0.05$ . CXCR7, CXC chemokine receptor-7; siRNAs, small interfering RNAs; qPCR, quantitative polymerase chain reaction; GAPDH, glyceraldehyde 3-phosphate dehydrogenase; LTS, laryngotracheal stenosis; SD, standard deviation.

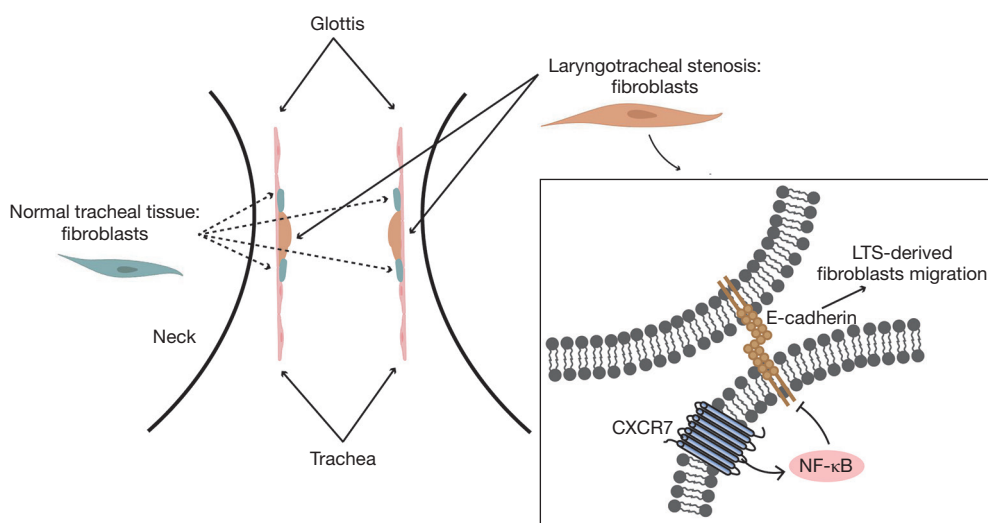


**Figure 5** A schematic diagram of the function of *CXCR7* in the fibroblasts derived from LTS compared with normal tracheal tissue. *CXCR7*, CXC chemokine receptor-7; LTS, laryngotracheal stenosis.

the phosphorylation of ERK and NF- $\kappa$ B P65 *in vitro* (26). In head and neck squamous cell carcinoma cells, *CXCR7* overexpression was also found to enhance the migration of by upregulating TGF- $\beta$ 1/Smad2/3 signaling pathway (16). The authors also found that *CXCR7* induced epithelial-mesenchymal transition through TGF- $\beta$ 1/Smad2/3 signaling pathway. However, in our previous work (10), we showed that there were no significant differences in the protein expressions of SMAD4 and phospho-SMAD2/3, suggesting that the TGF- $\beta$ /Smad signaling pathway was not activated. In pulmonary capillary endothelial cells, *CXCR7* overexpression decreased TGF- $\beta$ 1-induced collagen production and the expression of  $\alpha$ -SMA by blocking the Jag1-Notch pathway. The inhibition of *CXCR7* resulted in a persistent upregulation of the Jag1-Notch signaling pathway (12). In human umbilical vein endothelial cells in the process of angiogenesis, upregulated *CXCR7* was found to inhibit the expression of  $\alpha$ -SMA and activate AKT and ERK signaling pathways, while simultaneously suppressing Wnt/ $\beta$ -catenin pathways (13). In sum, *CXCR7* could activate various signaling pathways such as ERK, NF- $\kappa$ B, Wnt/ $\beta$ -catenin, TGF- $\beta$ /Smad or Jag1-Notch, inducing kinds of effector such as  $\alpha$ -SMA or E-cadherin, and eventually different biological functions in specific cells or circumstances. It deserves further research to uncover the underlying factors that control the downstream signaling pathways of *CXCR7* in certain cells or conditions. Nevertheless, the study has limitations relating to experimental model and translatability. The sample size

of the study is relatively small. And cell culture can result in loss of context cues and alter gene expression and other attributes of *in situ* tissues. Additionally, there may have been confounders if the experimental tissues in the LTS and normal group were not matched optimally. What is more, the role of *CXCR7*-related pathways in LTS should not only be demonstrated at the cellular level, but also be verified by further animal experiments and clinical trials.

## Conclusions

LTS had an increased *CXCR7* expression but decreased *E-cadherin* expression *in vivo* and *in vitro* fibroblasts. *CXCR7* agonist could inhibit *E-cadherin* expression by activating NF- $\kappa$ B signaling pathway and thereby promotes LTS derived fibroblasts' migration, which may contribute to the pathogenesis of fibrosis in LTS.

## Acknowledgments

**Funding:** This study was supported by National Natural Science Foundation of China (No. 82272270); and the Science and Technology Commission of Shanghai Municipality Funds (Nos. 22ZR1451700 and 21ZR1452800).

## Footnote

**Reporting Checklist:** The authors have completed the MDAR

reporting checklist. Available at <https://tp.amegroups.com/article/view/10.21037/tp-23-118/rc>

*Data Sharing Statement:* Available at <https://tp.amegroups.com/article/view/10.21037/tp-23-118/dss>

*Peer Review File:* Available at <https://tp.amegroups.com/article/view/10.21037/tp-23-118/prf>

*Conflicts of Interest:* All authors have completed the ICMJE uniform disclosure form (available at <https://tp.amegroups.com/article/view/10.21037/tp-23-118/coif>). The authors have no conflicts of interest to declare.

*Ethical Statement:* The authors are accountable for all aspects of the work in ensuring that questions related to the accuracy or integrity of any part of the work are appropriately investigated and resolved. The study was conducted in accordance with the Declaration of Helsinki (as revised in 2013). The study was approved by Committees of human ethics and experimental safety of Shanghai Children's Hospital (No. 2019R065) and informed consent was taken from the patients' guardians.

*Open Access Statement:* This is an Open Access article distributed in accordance with the Creative Commons Attribution-NonCommercial-NoDerivs 4.0 International License (CC BY-NC-ND 4.0), which permits the non-commercial replication and distribution of the article with the strict proviso that no changes or edits are made and the original work is properly cited (including links to both the formal publication through the relevant DOI and the license). See: <https://creativecommons.org/licenses/by-nc-nd/4.0/>.

## References

- Smith MM, Buck LS. Update on the diagnosis and management of pediatric laryngotracheal stenosis. *Expert Rev Respir Med* 2022;16:1035-41.
- Murphy MK, Motz KM, Ding D, et al. Targeting metabolic abnormalities to reverse fibrosis in iatrogenic laryngotracheal stenosis. *Laryngoscope* 2018;128:E59-67.
- Hillel AT, Ding D, Samad I, et al. T-Helper 2 Lymphocyte Immunophenotype Is Associated With Iatrogenic Laryngotracheal Stenosis. *Laryngoscope* 2019;129:177-86.
- Motz K, Samad I, Yin LX, et al. Interferon- $\gamma$  Treatment of Human Laryngotracheal Stenosis-Derived Fibroblasts. *JAMA Otolaryngol Head Neck Surg* 2017;143:1134-40.
- Antón-Pacheco JL, Usategui A, Martínez I, et al. TGF- $\beta$  antagonist attenuates fibrosis but not luminal narrowing in experimental tracheal stenosis. *Laryngoscope* 2017;127:561-7.
- Shook BA, Wasko RR, Rivera-Gonzalez GC, et al. Myofibroblast proliferation and heterogeneity are supported by macrophages during skin repair. *Science* 2018;362:eaar2971.
- Guerrero-Juarez CF, Dedhia PH, Jin S, et al. Single-cell analysis reveals fibroblast heterogeneity and myeloid-derived adipocyte progenitors in murine skin wounds. *Nat Commun* 2019;10:650.
- Lynch MD, Watt FM. Fibroblast heterogeneity: implications for human disease. *J Clin Invest* 2018;128:26-35.
- Kotaru C, Schoonover KJ, Trudeau JB, et al. Regional fibroblast heterogeneity in the lung: implications for remodeling. *Am J Respir Crit Care Med* 2006;173:1208-15.
- Hu B, Wang J, Chen J, et al. The heterogeneity of fibroblasts in laryngotracheal stenosis and skin hypertrophic scar in pediatric patients. *Int J Pediatr Otorhinolaryngol* 2021;145:110709.
- Guan S, Zhou J. CXCR7 attenuates the TGF- $\beta$ -induced endothelial-to-mesenchymal transition and pulmonary fibrosis. *Mol Biosyst* 2017;13:2116-24.
- Cao Z, Lis R, Ginsberg M, et al. Targeting of the pulmonary capillary vascular niche promotes lung alveolar repair and ameliorates fibrosis. *Nat Med* 2016;22:154-62.
- Shen M, Feng Y, Wang J, et al. CXCR7 Inhibits Fibrosis via Wnt/ $\beta$ -Catenin Pathways during the Process of Angiogenesis in Human Umbilical Vein Endothelial Cells. *Biomed Res Int* 2020;2020:1216926.
- Buskermolen JK, Roffel S, Gibbs S. Stimulation of oral fibroblast chemokine receptors identifies CCR3 and CCR4 as potential wound healing targets. *J Cell Physiol* 2017;232:2996-3005.
- Wu YC, Tang SJ, Sun GH, et al. CXCR7 mediates TGF $\beta$ 1-promoted EMT and tumor-initiating features in lung cancer. *Oncogene* 2016;35:2123-32.
- Kim N, Ryu H, Kim S, et al. CXCR7 promotes migration and invasion in head and neck squamous cell carcinoma by upregulating TGF- $\beta$ 1/Smad2/3 signaling. *Sci Rep* 2019;9:18100.
- Li R, Guan Z, Bi S, et al. The proton-activated G protein-coupled receptor GPR4 regulates the development of osteoarthritis via modulating CXCL12/CXCR7 signaling. *Cell Death Dis* 2022;13:152.
- Grimaldi C, Schumacher I, Boquet-Pujadas A, et al.

- E-cadherin focuses protrusion formation at the front of migrating cells by impeding actin flow. *Nat Commun* 2020;11:5397.
19. Cai D, Chen SC, Prasad M, et al. Mechanical feedback through E-cadherin promotes direction sensing during collective cell migration. *Cell* 2014;157:1146-59.
  20. Kuang L, Wu J, Su N, et al. FGFR3 deficiency enhances CXCL12-dependent chemotaxis of macrophages via upregulating CXCR7 and aggravates joint destruction in mice. *Ann Rheum Dis* 2020;79:112-22.
  21. Nguyen HT, Reyes-Alcaraz A, Yong HJ, et al. CXCR7: a  $\beta$ -arrestin-biased receptor that potentiates cell migration and recruits  $\beta$ -arrestin2 exclusively through G $\beta$  subunits and GRK2. *Cell Biosci* 2020;10:134.
  22. Décaillot FM, Kazmi MA, Lin Y, et al. CXCR7/CXCR4 heterodimer constitutively recruits beta-arrestin to enhance cell migration. *J Biol Chem* 2011;286:32188-97.
  23. Zhou H, Tu Q, Zhang Y, et al. Shear stress improves the endothelial progenitor cell function via the CXCR7/ERK pathway axis in the coronary artery disease cases. *BMC Cardiovasc Disord* 2020;20:403.
  24. Ngamsri KC, Müller A, Bösmüller H, et al. The Pivotal Role of CXCR7 in Stabilization of the Pulmonary Epithelial Barrier in Acute Pulmonary Inflammation. *J Immunol* 2017;198:2403-13.
  25. Zhao K, Yao Y, Luo X, et al. LYG-202 inhibits activation of endothelial cells and angiogenesis through CXCL12/CXCR7 pathway in breast cancer. *Carcinogenesis* 2018;39:588-600.
  26. Ngamsri KC, Jans C, Putri RA, et al. Inhibition of CXCR4 and CXCR7 Is Protective in Acute Peritoneal Inflammation. *Front Immunol* 2020;11:407.

**Cite this article as:** Xu M, Hu B, Chen J, Zhao L, Wang J, Li X. CXCR7 promotes the migration of fibroblasts derived from patients with acquired laryngotracheal stenosis by NF- $\kappa$ B signaling. *Transl Pediatr* 2023;12(9):1634-1645. doi: 10.21037/tp-23-118